Urban growth pattern with urban flood and temperature vulnerability using AI: a case study of Delhi

Gaurav S[1], Shafia A[1]and Bharath H A[1,*]

[1]Ranbir and Chitra Gupta School of Infrastructure Design and Management, Indian Institute of Technology Kharagpur, West Bengal- 721302, India

bhaithal@iitkgp.ac.in

Abstract. Urbanisation and its growth patterns are attribute of spatio-temporal changes in an area. Rapid and irreversible urbanization is the primary driver in changing landscape dynamics of the urban areas causing significant damage to the natural ecosystems. Cities in India are experiencing extensive urban growth and change through increasing population, changing social aspects, geographical influence, and increased complexity. This paper aims at modelling urban expansion through agent-based analysis considering the effect on the phenomenon of urban flood and urban heat island formation. Urban pattern analysis was analysed using temporal remote sensing data for the period 2003-2017. The results obtained depict that urban footprint has increased by 49.7% whereas vegetation has decreased by 27% in the study region. The study also identified various zones vulnerable to urban flood and land surface temperature variation in the region. This analysis would aid in managing urban stress and irreversible damages that it may cause to the environment through structural and non-structural measures, which can significantly help in sustainable management of natural resources.

1. Introduction

Urbanization is a dynamic process which is often perceived in terms of demographic, social, political and economic growth of a society. Urbanization causes massive alterations in environment at regional to global scales [1]. Unplanned and rapid urbanization across the globe has caused extensive transformation in ecological process of the environment including biodiversity losses, green-house gas emissions, ecosystem services, water quality, etc., elevating the vulnerability of urban areas [2, 3]. It is due to rapid urbanization that majority of the cities experience huge demographic pressure which results in urban sprawl. Unplanned and dispersed growth at urban fringes is termed as urban sprawl [4]. It takes place in the peri-urban areas in the circular form or extended urban development [5-7]. This is a challenge to city management for providing basic infrastructure and amenities [8].

Unplanned urbanization, temporal change in land use patterns leads to a variety of environmental problems, some of which have been studied in various researches across the globe including urban sprawl, urban flood and formation of surface urban heat island. For instance, globally researchers have discussed many significant impacts of urbanization leading to an intensification of intensity and magnitude of floods. According to Alaghmand et al. [9], urbanization leads to a number of changes in hydrological characteristics of any catchment area such as decreased infiltration, increase in runoff, increase in frequency and flood height. Subsequent drainage problems are caused by significant increase in impermeable area, without reference to a catchment's natural runoff characteristics [10] that would make it six times more vulnerable [11]. Conversion of water bodies to residential layouts as

compounded the problem by removing the interconnectivities in an undulating terrain [12, 13]. Similarly, researchers have also explained that the increase in impervious layers and loss of vegetative cover leads to urban heat islands (UHI) where these areas experience higher temperature than immediate rural regions. Higher temperature surrounded by comparatively cool temperature forms phenomena of urban heat island [14]. Land Surface Temperature (LST) is considered as main pointer of urban heat island, defined as the radiative skin temperature of the land surface, as measured in the direction of the remote sensor. The consequences of UHI include increased emission of greenhouse gases and air pollutants, increased energy consumption and many other direct and indirect impact on environment.

Remote Sensing (RS) has been the recently developed cost-effective mechanism of data acquisition. In recent years, remotely sensed data has been widely used in natural resource mapping and as input for modeling of various environmental processes. RS data along with Geographic Information System (GIS) are used in solving many problems in urban planning. For example, expansions of urban areas, Bharath & Ramachandra [15] studied seven tier II cities of Karnataka using an cohesive methods of geospatial approach combining RS and GIS. Sudhira et al. [5] analyzed the spatiotemporal dynamics of the urbanization using RS in Mangalore. Various research on urban floods using RS have been done. Sowmya et al. [16] identified vulnerability zones to urban flood in Cochin City using Multi-Criteria Evaluation Approach (MCEA) in GIS. Similarly, Elsheikh et al. [17] integrated GIS with MCEA to investigate flood risk using rainfall, drainage, etc. Sadeghi et al. [18] applied a key index towards flood vulnerability mapping in Iran. Similarly, RS and GIS has been widely used to understand UHI phenomena. El-Hattab et al. [19] investigated relation between UHI and LST, and mapped UHI intensity using Landsat thermal band for Cairo and Giza Cities. Gaur et al. [20] used city setting characteristics towards shaping their future UHI scenarios for 20 Canadian cities.

In this backdrop, the extent of all these problems have been analyzed for Delhi metropolitan region in this communication with the following objectives: i) To understand land use pattern change using RS data through spatial metrics and circular-gradients, ii) Identification of various zones vulnerable to urban flooding, iii) Quantification of LST to understand the underlying dynamics of UHI.

2. Study Area

Delhi metropolitan region has been considered for study. Delhi is the largest metropolis with high population density in India. Located at 28.61° N lat. & 77.23°E long. Census 2011 tabulates population of Delhi as 16 million with of 1483 km2.It also states that in period of 2001-2011, total number of urban population increased by 97.5%. Figure 1 represents boundary of Delhi with 10km buffer to analyze the growth of peri-urban areas

3. Data Used

Data used is a tabulated in Table 1. Satellite data from Landsat series were acquired from public domains. Toposheets were used to extract boundary maps.

Table 1. Data used for study.

DATA USED	PURPOSE
Landsat (30m): L-5(TM) and L-8(OLI) data	Land cover and land use analysis
ASTER DEM	Terrain analysis and Drainage map extraction
Toposheets of1:50000 and 1:250000 scales	Generate boundary and base layer maps
ISRO - Bhuvan and Google Earth	Verification and preparation of base layers including boundary
Field visit data – captured using GPS	Geo-correcting and generating validation dataset

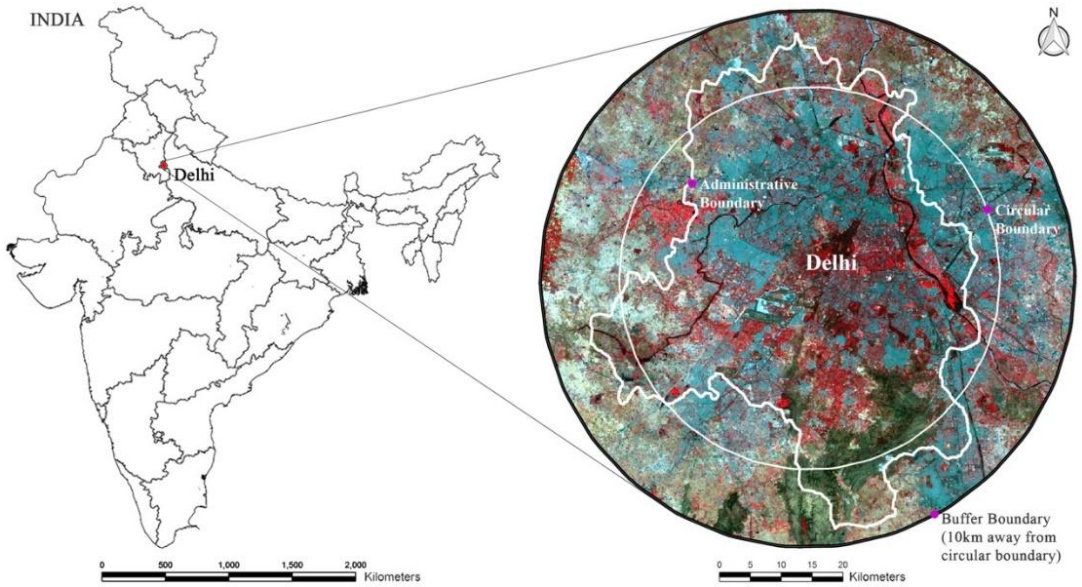

Figure 1. Administrative boundary of Delhi & buffer boundary taken for study.

4. Method

Time series spatial data was acquired for the period 2003-2017 to understand urban dynamics. Remote sensing data (Landsat series) for different time period was acquired from United States Geological Survey (USGS) Earth Explorer). A multistep approach was adopted, as illustrated in figure 2 in order to achieve the aforementioned objectives.

4.1. *Data Pre-processing*

The remote sensing data obtained were, geo-corrected, rectified [21] and cropped pertaining to the study area. Geo-registration of remote sensing data (Landsat data) has been done using ground control points collected from the field using pre-calibrated Global Positioning System (GPS) and also from known points (such as road intersections, etc.) collected from geo-referenced topographic maps.

4.2. Land Cover and Land Use Dynamics

Physical characteristics of the earth's surface such as water, vegetation, soil and other physical features can be defined as Land Cover while Land Use refers to the way land has been used for settlements concerning social, economic and cultural purposes by humans [22]. To quantify percentage of the vegetation cover, Normalized Difference Vegetation Index (NDVI). was computed Its value ranges from values -1 to +1. High values of NDVI indicate thick canopy vegetation (0.6 to 0.8), moderate values represent low density vegetation (0.1 to 0.3) and low values (-0.1 and below) correspond to soil or barren areas of rock, sand, or urban built-up. It is extracted from the NIR (near infrared) and Red (visible) band of the electromagnetic spectrum using equation (1):

$$NDVI = \frac{NIR\ (DN) - RED\ (DN)}{NIR\ (DN) + RED\ (DN)} \quad (1)$$

Further to investigate the usage of land due to anthropogenic activities, land use analysis was performed. It involves categorizing each pixel in the spatial data into different land use themes such as water bodies, vegetation, built up and others (that includes barren lands, etc.). Land use analysis was carried out using supervised pattern classifier named Gaussian Maximum Likelihood Classifier (GMLC). Data was classified using signatures from training sites that include four land use classes viz., urban, vegetation, water and others. Performance of classifiers is evaluated using accuracy assessment method such as overall accuracy and kappa statistics [23].

4.3. Urban Sprawl Quantification using Gradient Analysis and Spatial Metrics

In any urban area, the pattern of urbanization is not uniform in all directions. In order to understand the growth pattern, the region has been divided into 4 zones based on directions- Northwest (NW), Northeast (NE), Southwest (SW) and Southeast (SE) respectively. Each zone was further divided into concentric circles of 1km radius from the centre of the city. Further, urban growth for each circle was computed zone wise using various Landscape metrics for different periods as described in Table 2.

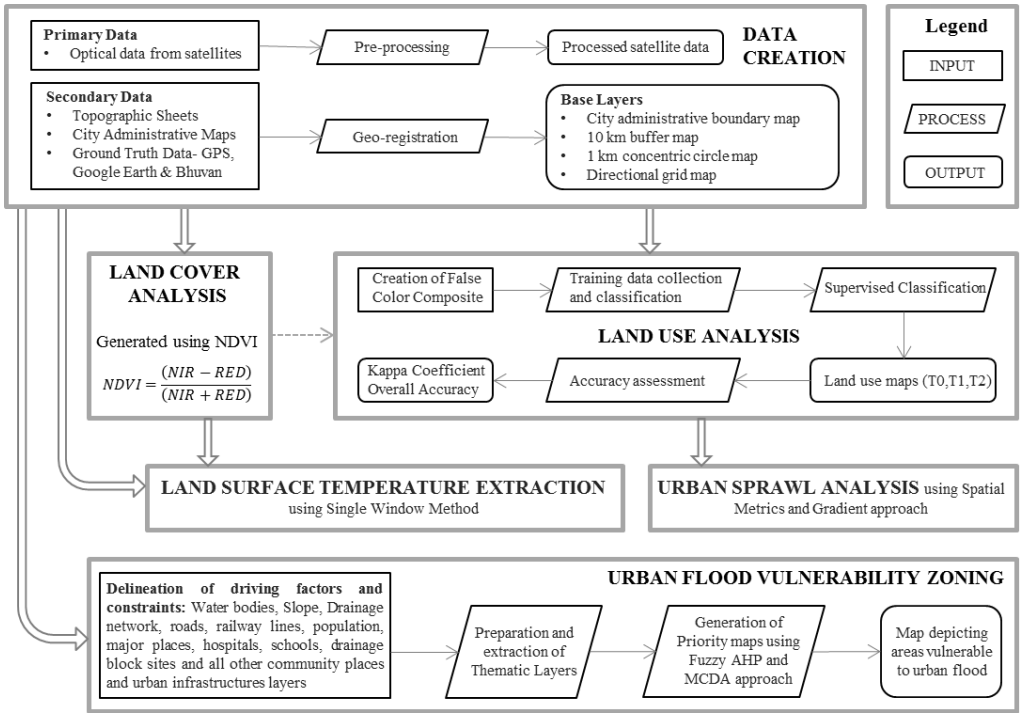

Figure 2. Method adopted for analysis.

Table 2. Landscape metrics calculated in the analysis.

Indicator	Formula
Number of patches (NP)	$NP = n_i$, Range: NP ≥ 1 n_i = number of patches in the landscape of patch type i
Clumpiness index(Clumpy)	$CLUMPY = \left(\left[\frac{G_i - P_i}{P_i}\right], for\ G_i < P_i P_i < 5; else\ \frac{G_i - P_i}{1P_i}\right)$ g_{ii} = like adjacencies between pixels of patch i - double-count method, g_{ik} = adjacencies (joins) between pixels of patch types i and k -double-count method, min-e_i = minimum perimeter. Range: [−1,1]
Normalized landscape shape index (NLSI)	$NLSI = \frac{e_i - \min e_i}{\max e_i - \min e_i}$ e_i = total length of edge (or perimeter), Range: 0 to 1

4.4. Urban Flood Vulnerability Zoning

Multi-temporal satellite data and other spatial data sources collected were used for delineation of various influencing thematic layers. Remotely acquired Digital Elevation Maps (DEM) was used for extraction of slope and natural drainage pattern. Water bodies and artificial drainage layers were obtained from maps of landuse classification and used as influencing layer. Natural drain block sites

were marked by overlaying natural drainage layer on classified land use map. These influencing marked block sites along with major water-logged areas in the study region obtained from Delhi traffic police data source [24] were mapped using data collected during field visit and ground truth studies carried out using GPS. Tabular population data was collected from Census of India [25]. Ward map of every area within study region was delineated using Bhuvan and population dataset was linked to it in order to derive the influencing raster layer of population density. Other influencing layers of i) social amenities including schools, colleges and hospitals, ii) community areas including parks, religious and political places, (iii) urban infrastructure layers including rail & road network and industries, were digitized using Google earth.

Further, distance maps were generated for all the above-mentioned influencing layers. Fuzzy approach was used for these distance maps to normalize data values and assign random values ranging from 0 to 255, where 0 signifies nearest distance to an influencing factor and 255 the farthest distance from it. These normalized influencing layers were then taken as inputs to Analytical Hierarchical Process (AHP) to assign weights to each of the layers. Each factor is compared with another in pair wise comparison followed by enumeration of consistency ratio which should be preferably less than 0.1 for the consistency matrix to be acceptable. Generation of vulnerability map was done by integrating the layers prepared through Multi-Criteria Decision Analysis (MCDA) approach which combines various criteria into a single index that indicates vulnerability in the study area for given datasets as inputs. The vulnerability output thus generated was then reclassified into four ranges and zones viz., low, moderate, high and very high vulnerabilities.

4.5. Quantification of Land Surface Temperature (LST)

The single TIR channel method was adopted for extraction of LST from acquired satellite data. It uses the radiance measured by the satellite sensor in a single channel, chosen within an atmospheric window, and corrects the radiance for residual atmospheric attenuation and emission. LST is then retrieved from the radiance measured in this channel by inverting the radiative transfer equation (RTE) as explained in Table 3.

Table 3. Process of Land Surface Temperature Extraction.

LST Extraction	Formula	Description
Conversion of DN into Spectral Radiance	$L_\lambda = (Gain * DN) + Offset$	L_λ = spectral radiance, *Gain*= band specific multiplicative rescaling factor obtained from metadata, *Offset* = band specific additive rescaling factor obtained from metadata.
Conversion of Spectral Radiance into Temperature	$T_B = \frac{K_2}{\ln\left(\frac{K_1}{L_\lambda}+1\right)}$	T_B = At-satellite brightness temperature (Kelvin), K_1 = calibration constant (607.76 for Landsat 5 and 480.88 for Landsat 8), K_2 = calibration constant (1260.56for Landsat 5 and 1201.14 for Landsat 8).
Calculation of Land Surface Temperature	$LST = \frac{T_B}{1+\left(\frac{\lambda T_B}{\rho} X \ln(\varepsilon)\right)}; \left(\rho = \frac{hc}{\sigma} = 1.438\, X\, 10^{-2} mK\right)$	λ = mean wavelength of the thermal band, ε = emissivity of the element *h*= Plank's constant, c = speed of light σ= Stefan Boltzmann constant

5. Results and Discussions

5.1. Land Cover Analysis

Temporal vegetation cover analysis done through the computation of NDVI as shown in Figure 3. It depicts the land cover of the study region during 2003, 2010 and 2017. Temporal analyses indicate decline in green spaces like reserve forest areas, parks, plantations, conserved areas, etc. by 22.9% for the period 2003-2017 in the NCT region. Table 4 indicates the temporal NDVI values, highlighting the decline of area under vegetation.

5.2. Land Use Analysis

Land use temporal distribution was computed using Gaussian maximum likelihood classifier as discussed. Figure 4 depicts the temporal land use changes in NCT during 2003-2017 and Table 4 depicts the area under different land use classes. The overall accuracy of the classified images was 91%, 88% and 94% for the year 2003, 2010 and 2017 respectively which were in confirmation with obtained kappa statistics of 0.86, 0.82 and 0.91. Land use analysis reveals the increase in the urban area from 21.26% in 2003 to 32.37% in 2017.

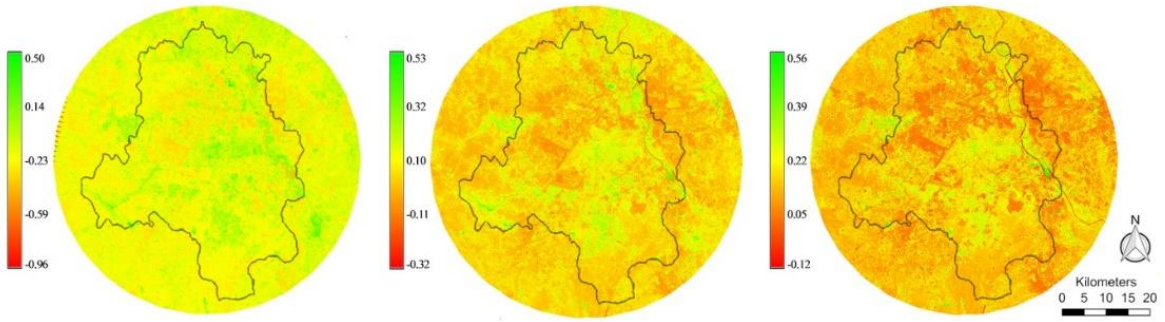

Figure 3. Temporal Land Cover in the study region for the time period 2003-2017.

This result can directly be linked with Delhi's elevating population density and 2011 Census which states that population in urban areas in Delhi is around 97%. The vegetation area decreased from 30.16% in 2003 to 20.03% in 2017 which can be a direct outcome of growing urban footprint in the region and related anthropogenic activities. Results also depicted that water bodies have reduced from 1.24% to 1.01% which reveals various encroachments in floodplains of river Yamuna. Changes in other category suggest the rapid transformation of agriculture and barren landscape to highly paved built up regions.

Table 4. Land Cover and Land Use statistics of the study region for the time period 2003-2017.

Year	LAND COVER		LAND USE			
	Vegetation	**Non- vegetation**	**Urban**	**Vegetation**	**Water**	**Others**
2003	37.26	62.74	21.26	30.16	1.24	46.97
2010	33.87	66.13	26.83	28.16	1.17	43.84
2017	28.74	71.26	32.37	22.03	1.01	44.59

5.3. Spatial metrics analysis

The results from land use classification along with gradient and zonal layers were taken as input to obtain spatial metrics. Some of the metrics generated are as follows:

- No. of patches (NP): This metrics is an indicator of degree of fragmentation in a given study region. Values close to zero indicates a compact and aggregated growth while the higher values indicate fragmented growth. In Figure 5, city centre has value very close to 0 indicating a compact and dense core in 2017, while the city is having more fragmented growth as we move towards the buffer region
- Clumpiness index (Clumpy): It gives the degree of aggregation and disaggregation in a given area with values ranging from 0 to 1. Values closer to 1 depict an aggregated and compact growth while values closer to 0 indicates scattered and fragmented growth. Figure 6 shows the core city values close to 1 in all the four zones because of the dense and compact core while there is decreasing trend towards the buffer region in all the three years as the patches are randomly placed.

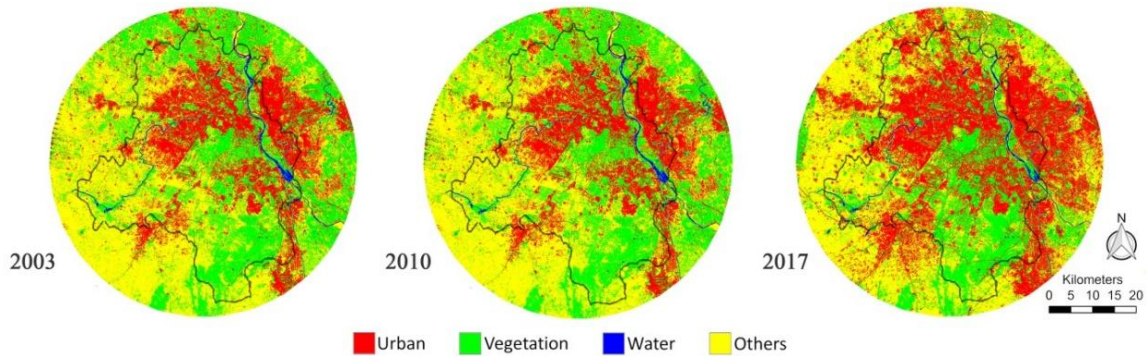

Figure 4. Temporal Land Use in the study region for the time period 2003-2017.

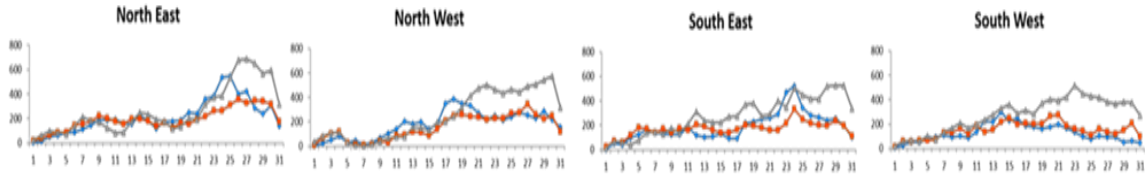

Figure 5. No. of patches (NP).

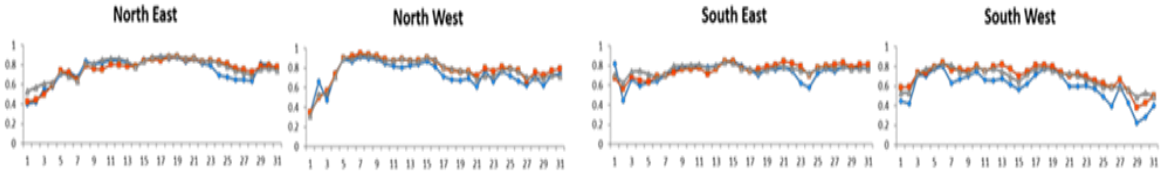

Figure 6. Clumpiness index (Clumpy)

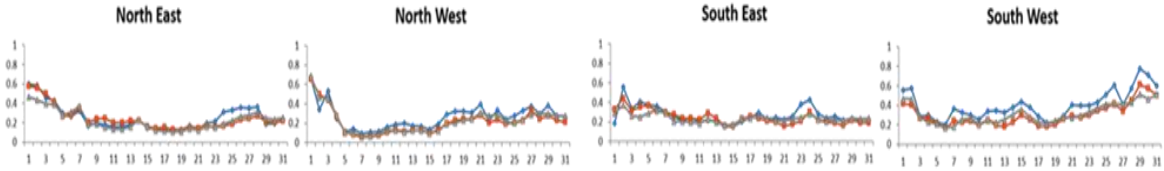

Figure 7. Normalized Landscape shape index (NLSI).

Normalized Landscape shape index (NLSI): It is an indicator of aggregation or disaggregation in a particular class with respect to shape, meaning, land use of simple and compact shapes has values close to 0 while the values increase with the complexity of the shapes to maximum being 1. Figure 7 shows values close to 0 in city centre due to compact and aggregated built up while the buffer regions show higher values depicting the presence of more complex shapes and disaggregated growth. In 2017, there is an increasing trend towards the buffer indicating the simple and aggregated city centre and fragmented and disaggregated peri-urban regions.

5.4. Urban Flood Vulnerability Zoning

Layers influencing urban flood including driving factors and constraints were extracted as discussed and are represented in Figure 8. Consistency ratio of 0.03 was achieved, considered to be acceptable and reliable to continue further analysis. Multi-Criteria Decision Analysis (MCDA) technique was applied for vulnerability zoning using all the influencing layers along with respective weights obtained by AHP and slope used as a constraint. The final vulnerable map for NCT region was thus obtained as depicted in Figure 8. The four vulnerability zones such as low, moderate, high and very high generated

show that very high and high vulnerable zones together constituted 45.4 (1180 km^2) of the total area of the study region and 36.38% of the total area has low urban flood vulnerability. Some of the areas falling under very high and high zones are Sahibabad Industrial area, Indirapuram and Karkardooma in NE gradient; Patparganj, Faridabad,Okhla and Hauz Khas in SE gradient; Indira Gandhi International Airport, Sector 7 and 8 of Gurgaon in SW gradient; Rohini, Uttamnagar, Paschim Vihar and Janakpuri in NW gradient.

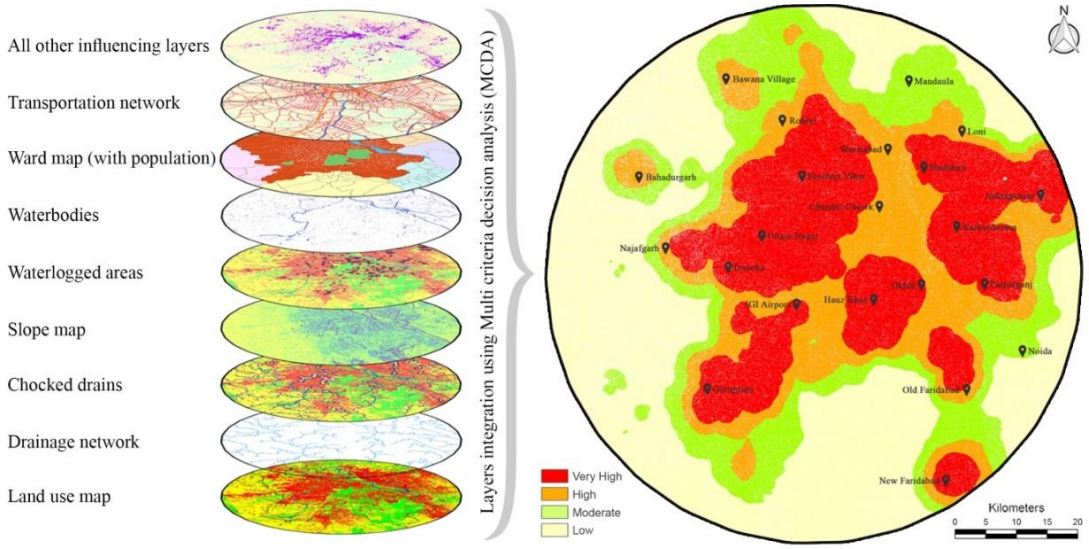

Figure 8. Influencing layers generated and urban flood vulnerability zones identified in study region.

5.5. Land Surface Temperature

Land surface temperature was quantified using single window technique for the period 2003-2017 as shown in Figure 9. Mean temperature of the study area has rapidly increased from 25˚C in 2003 to 39˚C in 2010 and 41˚C in 2017. Some of the areas have experienced significant changes in land surface temperature due to conversion of land use type like vegetation to urban area. Four separate regions in the study area have been considered to understand the temperature fluctuations with respect to various land use classes during the study period.

Temperature profile for the A) Airport, B) Wazirabad, C) Shastri Nagar and D) Jehangirpuri are as shown in figure 10. In case of Airport, the airstrip and the airport building show the highest temperature while as we move away the temperature starts to descend because of presence of some vegetated surfaces. Similarly, in case of Wazirabad and Jehangirpuri presence of compact urban patch shows significant rise in the temperature graph while in Shastri Nagar land surface temperature profile has completely changed due to the encroachment near the Yamuna river.

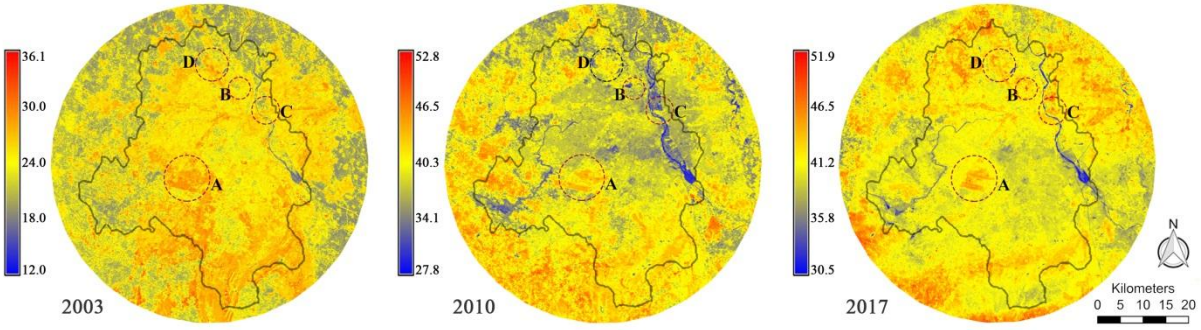

Figure 9. Maps depicting Land surface temperature in the study region.

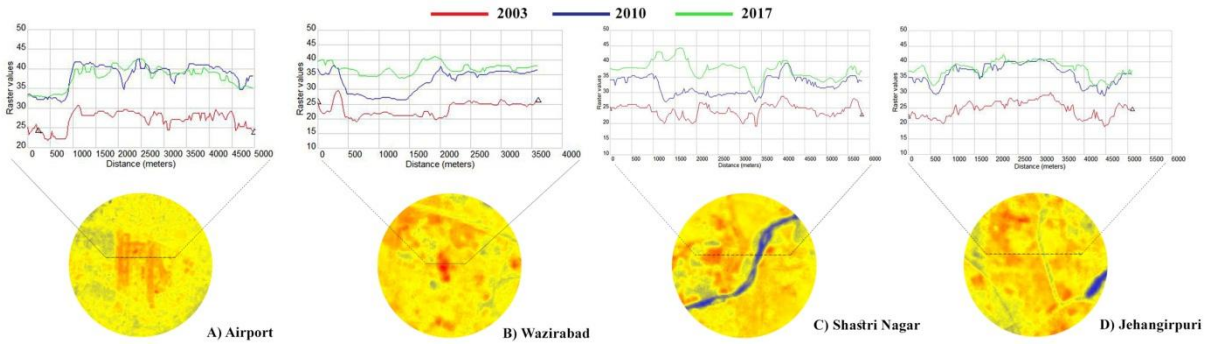

Figure 10. Temperature profile of A) Airport, B) Wazirabad, C) Shastri Nagar and D) Jehangirpuri.

6. Conclusion

Temporal land cover analysis indicates a decline in vegetation cover by about 23%, while the non-vegetation area has increased by about 13.6%. Natural green spaces and open grounds have decreased dramatically within the core city in terms of parks and wetland areas whereas agricultural fields have been converted to built-up areas in the NCT region. Land use analysis for the period 2003-2017 indicate that the built-up area has increased from 21.26% to 32.37%. The extent of urbanization has been analysed by quantifying urban sprawl considering metrics like number of patches, shape, clumpiness and interspersion/ juxtaposition. This investigation revealed that densification has happened around the city centre and has spread out towards fringes from 2003 to 2017. The development in core areas is compact, aggregated and well interspersed, whereas in the peri-urban areas, development is fragmented, disaggregated and poorly distributed. These results depicting rapid urban growth can be directly linked to the urban flood vulnerable zones identified in the study region where a large percentage of the urban core is falling under high vulnerability zone. Similar observation was made in LST extraction where various places have experienced significant changes in land surface temperature due to conversion of land use type to urban. The study clearly depicts the extent of urbanization in NCT region and how adversely urban growth is transforming the region, leading to a variety of environmental issues. This communication would help the urban planners and city development authority in better understanding of the process and pattern of urbanization in the region and can play a vital role in future development and efficient planning and management of resources.

Acknowledgment

We are grateful to (i) SERB, India (ii) Asia Pacific Network (APN) (iii) Indian Institute of Technology, Kharagpur for financial and infrastructural support. We thank USGS Earth Resources Observation and Science (EROS) center for providing the environmental layers and Global Land Cover Facility (GLCF) for providing Landsat data. We thank Mr. Chandan M.C. and Mr. Nimish Gupta, Indian Institute of Technology, Kharagpur for their insightful help during the work.

References

[1] Huang, S., Taniguchi, M., Yamano, M., & Wang, C. H. (2009). Detecting urbanization effects on surface and subsurface thermal environment—A case study of Osaka. Science of the total environment, 407(9), 3142-3152.

[2] Singh, R.B., & Singh, S. (2007). Challenges of flood disaster management: a case study of Noida: a GIS approach. Disaster management: future challenges and opportunities, New Delhi: IKM Publications, 95-112.

[3] Sharma, R., & Joshi, P. K. (2016). Mapping environmental impacts of rapid urbanization in the National Capital Region of India using remote sensing inputs. Urban Climate, 15, 70-82.

[4] Ramachandra, T.V., Bharath, H.A., Sannadurgappa, D., (2012). Insights to Urban Dynamics through Landscape Spatial Pattern Analysis, Journal of Applied Earth Observation and Geoinformation. 18, 329-343.

[5] Sudhira, H. S., Ramachandra, T. V., & Jagadish, K. S. (2003). Urban sprawl: metrics, dynamics and modelling using GIS. International Journal of Applied Earth Observation and Geoinformation, 5(1), 29-39.
[6] Ramachandra, T.V., Bharath, H.A., Sowmyashree M. V., 2015. Monitoring urbanization and its implications in a mega city from space: Spatiotemporal patterns and its indicators, Journal of Environmental Management. 148, pp.67-91.
[7] Bharath, H.A., Chandan, M.C., Vinay, S., Gouri. H.A., Ramachandra, T.V., 2017. Green to gray: Silicon Valley of India, Journal of Environmental Management, accepted, in press.
[8] Ramachandra, T. V., & Kumar, U. (2008). Wetlands of greater Bangalore, India: automatic delineation through pattern classifiers. Electronic Green Journal, 1(26).
[9] Alaghmand, S., Bin Abdullah, R., Abustan, I., &Vosoogh, B. (2010). GIS-based river flood hazard mapping in urban area (a case study in Kayu Ara River Basin, Malaysia). International Journal of Engineering and Technology, 2(6), 488-500.
[10] Swan, A. (2010). How increased urbanization has induced flooding problems in the UK: A lesson for African cities?. Physics and Chemistry of the Earth, Parts A/B/C, 35(13), 643-647.
[11] Etuonovbe, A. K. (2011). The devastating effect of flooding in Nigeria. In FIG working week (Vol. 201, No. 1). Marrakech, Morocco: Bridging the Gap between Cultures.
[12] Ramachandra, T. V., Bharath, H.A., & Kumar, U. (2012). Conservation of wetlands to mitigate urban floods. Journal of Resources, Energy and Development, 9(1), 1-22.
[13] TERI, (2012). Mainstreaming Climate Resilience in Urban Areas- A case of Gorakhpur City.
[14] Bhargava, A., Lakmini, S., & Bhargava, S. (2017). Urban Heat Island Effect: It's Relevance in Urban Planning. Journal of Biodiversity & Endangered Species, 5(2).
[15] Bharath, H.A., & Ramachandra, T. V. (2013). Measuring urban sprawl in Tier II cities of Karnataka, India. In Global Humanitarian Technology Conference: South Asia Satellite (GHTC-SAS), 2013 IEEE (pp. 321-329). IEEE.
[16] Sowmya, K., John, C. M., &Shrivasthava, N. K. (2015). Urban flood vulnerability zoning of Cochin City, southwest coast of India, using remote sensing and GIS. Natural Hazards, 75(2), 1271-1286.
[17] Elsheikh, R. F. A., Ouerghi, S., &Elhag, A. R. (2015). Flood Risk Map Based on GIS, and Multi Criteria Techniques (Case Study Terengganu Malaysia). Journal of Geographic Information System, 7(04), 348.
[18] Sadeghi-Pouya, A., Nouri, J., Mansouri, N., & Kia-Lashaki, A. (2017). An indexing approach to assess flood vulnerability in the western coastal cities of Mazandaran, Iran. International Journal of Disaster Risk Reduction, 22, 304-316.
[19] El-Hattab, M., Amany, S. M., & Lamia, G. E. (2017). Monitoring and assessment of urban heat islands over the Southern region of Cairo Governorate, Egypt. The Egyptian Journal of Remote Sensing and Space Science.
[20] Gaur, A., Eichenbaum, M. K., &Simonovic, S. P. (2017). Analysis and modelling of surface Urban Heat Island in 20 Canadian cities under climate and land-cover change. Journal of environmental management, 206, 145-157.
[21] National Remote Sensing Centre, http://www.nrsc.gov.in Accessed on: November 10, 2017.
[22] Rawat, J. S., & Kumar, M. (2015). Monitoring land use/cover change using remote sensing and GIS techniques: A case study of Hawalbagh block, district Almora, Uttarakhand, India. The Egyptian Journal of Remote Sensing and Space Science, 18(1), 77-84.
[23] Mitrakis, N. E., Topaloglou, C. A., Alexandridis, T. K., Theocharis, J. B., & Zalidis, G. C. (2008). A novel self-organizing neuro-fuzzy multilayered classifier for land cover classification of a VHR image. International Journal of Remote Sensing, 29(14), 4061-4087.
[24] Delhi Traffic Police, https://delhitrafficpolice.nic.in/be-road- smart/water-logging-area-2/ Accessed on: October 29, 2017.
[25] Census of India. (2011). Available at: censusindia.gov.in/. Accessed on: November 10, 2017